Inorg. Chem. **1998,** *37,* 612−618

Articles

Iron(II) Complexes Containing the 1,2-Diphospholanoethane Ligand

Leslie D. Field,*,† Iain P. Thomas,† Trevor W. Hambley,‡ and Peter Turner‡

Divisions of Organic Chemistry and Inorganic Chemistry, School of Chemistry, University of Sydney, NSW 2006, Australia

Received February 20, 1997

The synthesis and crystal structure of *cis*-$Fe(BPE5)_2Cl_2$ (BPE5 = 1,2-diphospholanoethane), the first symmetrical *cis*-$Fe(PP)_2Cl_2$ (PP = bidentate phosphine), is reported (monoclinic, $P2_1/n$, $a = 12.084(3)$ Å, $b = 14.059(2)$ Å, $c = 17.665(2)$ Å, $\beta = 101.77(1)°$, $Z = 4$). The overall structure and Fe−P and Fe−Cl bond lengths of *cis*-$Fe(BPE5)_2Cl_2$ more closely resemble those in $Fe(PP_3)Cl_2$ complexes (PP_3 = tripodal, tetradentate phosphine ligand) than in other $Fe(PP)_2Cl_2$ complexes. In solution, *cis*-$Fe(BPE5)_2Cl_2$ exhibits temperature-dependent paramagnetic behavior due to reversible dissociation of chloride. The dissociation of chloride was exploited in the synthesis of $Fe(BPE5)_2X_2$ (X = Br, I) and $[Fe(BPE5)_2(L)(Cl)]^+$ (L = CO, PMe_3). The crystal structure of [*cis*-$Fe(BPE5)_2(CO)(Cl)][BPh_4]$ is reported (monoclinic, $P2_1/a$, $a = 12.938(3)$ Å, $b = 29.647(4)$ Å, $c = 13.131(3)$ Å, $\beta = 107.89(2)°$, $Z = 4$). The relative chelation strength of BPE5 in $Fe(PP)_2Cl_2$ complexes is BPE5 ≈ DMPE > DEPE > DPrPE [DMPE = 1,2-bis(dimethylphoshino)ethane; DEPE = 1,2-bis(diethylphoshino)ethane; DPrPE = bis(di-*n*-propylphosphino)ethane].

Introduction

The study of metal complexes of the MP_4X_2 type (M = Fe, Ru, Os; P = phosphine; X = halide, hydride) has been extensive, and the chemistry exhibited by metal phosphines depends to a large extent on the nature of the phosphine ligand(s) that they contain.[1] MP_4X_2 systems have been employed in many types of reactions including intramolecular[2] and intermolecular[3] C−H activation and as catalysts in organic synthesis.[4] The most frequently studied MP_4X_2 systems have incorporated two bidentate ligands (*e.g.* $R_2PCH_2CH_2PR_2$, R = Ph,[5] Me,[2a,3a−d,3f,6,7] and Et[8]).

To date, the existence of FeP_4Cl_2 complexes in which the chloride ligands occupy a *cis* geometry has only been observed when tetradentate phosphine ligands ($P((CH_2)_nPR_2)$: $n = 2, 3$; R = Ph,[9] Me,[3g,10] Cy[11]) have been used; *i.e.*, when the phosphines are constrained to occupy adjacent coordination sites. In this paper we report the synthesis of the first *cis*-FeP_4Cl_2 complex with two bidentate bisphosphines (PP), *cis*-$Fe(BPE5)_2Cl_2$ (***cis*-1**; BPE5 = 1,2-diphospholanoethane[12] (**2**)). The geometry adopted by ***cis*-1** is probably influenced by the steric bulk of the diphospholano ligands **2**.

Scheme 1

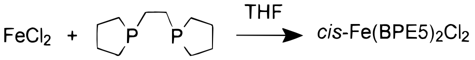

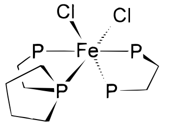

***cis* -1**

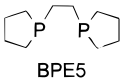

2

Results and Discussion

Synthesis of *cis*-$Fe(BPE5)_2Cl_2$ (*cis*-1). On addition of 2 equiv of BPE5 (**2**) to a THF solution of anhydrous iron(II) chloride, a burgundy solution formed, from which dark red crystals of *cis*-$Fe(BPE5)_2Cl_2$ (***cis*-1**) precipitated as the sole isolated product (Scheme 1). The complex ***cis*-1** is soluble in

---

[†] Division of Organic Chemistry.

[‡] Division of Inorganic Chemistry.

(1) See for example: Mayer, H. A.; Kaska, W. C. *Chem. Rev.* **1994**, 1239.

(2) (a) Jones, W. D.; Foster, G. P.; Putinas, J. M. *Inorg. Chem.* **1987**, *26*, 2120. (b) Antberg, M.; Dahlenberg, L. *Angew. Chem., Int. Ed. Engl.* **1986**, *25*, 260.

(3) (a) Jones, W. D.; Feher, F. *Organometallics* **1983**, *2*, 562. (b) Baker, M. V.; Field, L. D. *J. Am. Chem. Soc.* **1986**, *108*, 7433. (c) Baker, M. V.; Field, L. D. *J. Am. Chem. Soc.* **1986**, *108*, 7436. (d) Baker, M. V.; Field, L. D. *J. Am. Chem. Soc.* **1987**, *109*, 2825. (e) Antberg, M.; Dahlenberg, L.; Frosin, K. M.; Höck, N. *Chem. Ber.* **1988**, *121*, 859. (f) Field, L. D.; George, A. V.; Messerle, B. A. *J. Chem. Soc., Chem. Commun.* **1991**, *19*, 1339. (g) Bampos, N.; Field, L. D.; Messerle, B. A. *Organometallics* **1993**, *12*, 2529.

(4) (a) Jones, W. D.; Kosar, W. P. *J. Am. Chem. Soc.* **1986**, *108*, 5640. (b) Hsu, G. C.; Kosar, W. P.; Jones, W. D. *Organometallics* **1994**, *13*, 385.

(5) Hata, G.; Kondo, H.; Miyake, A. *J. Am. Chem. Soc.* **1968**, *90*, 2278.

(6) Chatt, J.; Watson, H. R. *J. Chem. Soc.* **1962**, 2545.

(7) Burn, M. J.; Fickes, M. G.; Hollander F. J.; Bergman, R. G. *Organometallics* **1995**, *14*, 137.

(8) Chatt, J.; Hayter, R. G. *J. Chem. Soc.* **1961**, 5507.

(9) (a) Bianchini, C.; Peruzzini, M.; Zanobini, F. *J. Organomet. Chem.* **1988**, 354, C19. (b) Bianchini, C.; Peruzzini, M.; Polo, A.; Vacca, A.; Zanobini, F. *Inorg. Chem.* **1991**, *30*, 279. (c) Bianchini, C.; Perez, P. J.; Peruzzini, M.; Zanobini, F.; Vacca, A. *Inorg. Chem.* **1991**, *30*, 279.

(10) (a) Bampos, N.; Field, L. D. *Inorg. Chem.* **1989**, *29*, 587. (b) Bampos, N.; Field, L. D.; Messerle, B. A. *Magn. Reson. Chem.* **1991**, *29*, 36.

(11) Jia, G.; Drouin, S. D.; Jessop, P. G.; Lough, A. J.; Morris, R. H. *Organometallics* **1993**, *12*, 906.

(12) Field, L. D.; Thomas, I. P. *Inorg. Chem.* **1996**, *35*, 2546.

S0020-1669(97)00192-4 CCC: $15.00

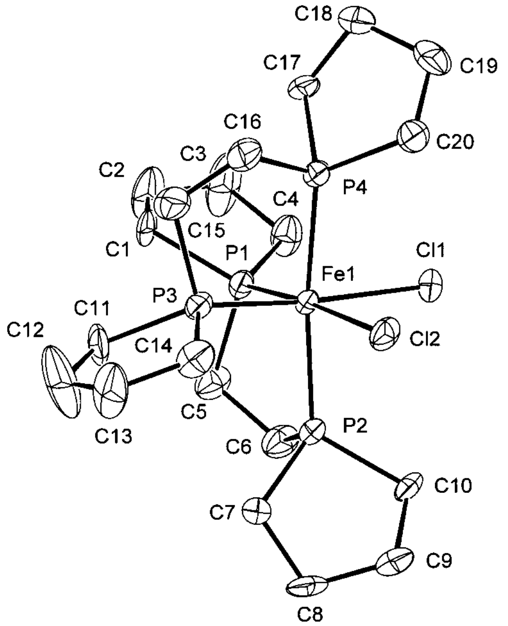

Figure 1. ORTEP plot (25% thermal ellipsoids, non-hydrogen atoms) of *cis*-Fe(BPE5)$_2$Cl$_2$ (***cis*-1**).

Table 1. Bond Lengths (Å) and Angles (deg) about the Iron Atom of *cis*-Fe(BPE5)$_2$Cl$_2$ (***cis*-1**)[a]

	Bond Lengths		
Fe−Cl(1)	2.384(3)	Fe−P(2)	2.225(3)
Fe−Cl(2)	2.403(3)	Fe−P(3)	2.185(3)
Fe−P(1)	2.181(3)	Fe−P(4)	2.223(3)
	Bond Angles		
Cl(1)−Fe−Cl(2)	89.4(1)	P(3)−Fe−P(4)	86.1(1)
Cl(1)−Fe−P(1)	88.4(1)	P(1)−Fe−P(4)	98.2(1)
Cl(1)−Fe−P(2)	87.1(1)	P(2)−Fe−P(3)	98.2(1)
Cl(1)−Fe−P(4)	88.4(1)	P(1)−Fe−P(3)	94.3(1)
P(1)−Fe−P(2)	86.5(1)	P(2)−Fe−P(4)	173.4(1)

[a] Errors in the least significant figures are presented in parentheses.

methanol, ethanol, and benzene but only sparingly soluble in THF. Recrystallization of ***cis*-1** from THF afforded crystals suitable for X-ray diffraction.

The ^{31}P{^{1}H} NMR spectrum of the filtered reaction mixture (recorded at 233 K) indicated that ***cis*-1** was the predominant product (two apparent triplets at 93.2 and 106.7 ppm, splitting = 40 Hz); a second product (91.8 ppm, singlet) is assigned as the isomeric *trans* complex *trans*-Fe(BPE5)$_2$Cl$_2$ (***trans*-1**; ~90:10 ***cis*-1**/***trans*-1**). On addition of *n*-hexane to the THF solution, a dark red solid precipitated, and this was insoluble in most organic solvents, including alcohols and THF. The product is probably oligomeric or polymeric but has not been further characterized. Attempts to isomerize pure ***cis*-1** to ***trans*-1** in refluxing methanol and benzene, by irradiation at ambient and low (233 K) temperatures, and by heating in the solid state were unsuccessful.

cis-Fe(BPE5)$_2$Cl$_2$ (***cis*-1**) crystallizes with 1 mol of THF as a slightly distorted octahedral complex in which the two chloride ligands are mutually *cis* (Figure 1). Selected structural data for complex ***cis*-1** are reported in Table 1. In comparison with related *trans*-Fe(PP)$_2$Cl$_2$ complexes [PP = DMPE (**3**),[13] DEPE (**4**),[13,14] DPrPE (**5**),[14] BPE6 (**6**),[15] BPE6 = 1,2-bis(1-phosphorinano)ethane; Table 2], the P−Fe−P chelation bite angle in ***cis*-1** is slightly wider (1−2°) and the Fe−P bond lengths shorter (~6%). The Fe−P bond lengths are short when *trans* to Cl, reflecting the weaker σ-donor ability of the chloride ligand. The *cis* disposition of the chloro ligands distinguishes ***cis*-1** from **3**−**6** and is presumably responsible for the distortion from octahedral geometry evident in Table 1. In ***cis*-1**, the BPE5 ligands interact significantly with the chlorine atoms and this undoubtedly contributes to the distortion from octahedral geometry.

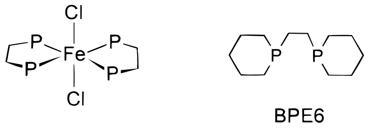

P P = $R_2PCH_2CH_2PR_2$
R = CH_3; DMPE **(3)**
R = CH_2CH_3; DEPE **(4)**
R = $CH_2CH_2CH_3$; DPrPE **(5)**
P P = BPE6 **(6)**

In complex ***cis*-1**, the Fe−Cl bonds are slightly longer than in complexes **3**−**6** but very similar to those of *cis*-Fe(P((CH$_2$)$_3$-PMe$_2$)$_3$)Cl$_2$ (**7**)[16] (Table 2). The chloride ligands of complexes ***cis*-1**, **7**, and **8** are all *trans* to strong σ-donor phosphine ligands, whereas, in complexes **3**−**6**, the two chloride ligands are mutually *trans*.

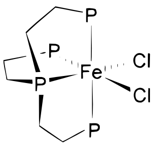

7

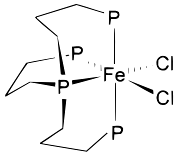

8

P(−P)$_3$ = P[(CH$_2$)$_2$PMe$_2$]$_3$ P(−P)$_3$ = P[(CH$_2$)$_3$PMe$_2$]$_3$

The phospholane rings at the two *trans* phosphines P(2) and P(4) of complex ***cis*-1** are in essentially envelope conformations (minimum torsion angles of 5.6 and 1°, respectively), in which the carbon atoms β to phosphorus (C(8) and C(18)) lie out of plane with respect to the rest of their respective rings. The ring at P(3) is the most planar (no torsion angle exceeds 11°), and the ring at P(1) is puckered.

Solution-State Temperature Dependent Paramagnetism of *cis*-Fe(BPE5)$_2$Cl$_2$ (*cis*-1). At room temperature, no signal was detected in the ^{31}P{^{1}H} NMR spectra of ***cis*-1** in either THF or methanol solution. However, on cooling, two broad resonances were observed, and at 233 K these were resolved as two sharp apparent triplets.

The broadness of the ^{31}P resonances of ***cis*-1** is due to paramagnetism probably originating from reversible dissociation of chloride to form a five-coordinate paramagnetic complex [Fe(BPE5)$_2$Cl]$^+$ (**9**). Methanol or THF solutions of ***cis*-1** which were saturated with sodium chloride gave well-resolved sharp signals in the ^{31}P{^{1}H} NMR spectra recorded at 300 K. Temperature-dependent paramagnetism has been observed for complexes **4** and **5** and in these complexes was attributed to reversible dissociation of one end of the bulky bidentate

---

(13) Di Vaira, M.; Midollini, S.; Sacconi, L. *Inorg. Chem.* **1981**, *20*, 3430.

(14) Baker, M. V.; Field, L. D.; Hambley, T. W. *Inorg. Chem.* **1988**, *27*, 2872−2876.

(15) Field, L. D.; Thomas, I. P.; Hambley, T. W.; Turner, P. Submitted for publication.

(16) Antberg, M.; Dahlenburg, L. *Inorg. Chim. Acta* **1985**, *104*, 51.

Table 2. Average Fe−Cl and Fe−P Bond Lengths (Å) and Chelate P−Fe−P Angles (deg) about the Iron Centers of $Fe(PP)_2Cl_2$ Complexes (***cis*-1**, **3**−**8**, and **15**)

	Fe−Cl	Fe−P[a]	Fe−P[b]	P−Fe−P[c]	ref
cis-$Fe(BPE5)_2Cl_2$ (***cis*-1**)	2.394[b,j]	2.183[j]	2.224[j]	86.3	this work
trans-$Fe(DMPE)_2Cl_2$ (**3**)	2.352(1)[a]	2.235[j]		85.8	13
trans-$Fe(DEPE)_2Cl_2$ (**4**)	2.344(1)[a]	2.260[j]		85.3	13,14
trans-$Fe(DPrPE)_2Cl_2$ (**5**)	2.345(2)[a]	2.268[j]		84.6	14
trans-$Fe(BPE6)_2Cl_2$ (**6**)	2.361(2)[a]	2.251[j]		85.2	15
cis-$Fe(P(CH_2)_3PMe_2)_3Cl_2$ (**7**)	2.388(5)[d] 2.410(4)[e]	2.202(5)[f] 2.231(5)[g]	2.322[g,h,j]	95.4, 97.1, 88.9	16
[*cis*-$Fe(BPE5)_2(CO)(Cl)]^+$ (**15**)	2.341[b,j]	2.237(8) 2.260(8)[i]	2.234[j]	85.7	this work

[a] *Trans* to chloride. [b] *Trans* to phosphorus. [c] Chelate angle. [d] *Trans* to apical phosphorus atom. [e] *Trans* to terminal phosphorus atom. [f] Apical phosphorus atom. [g] Terminal phosphorus atom. [h] Average of two mutually *trans* phosphorus atoms. [i] *Trans* to CO. [j] Average values.

phosphine ligand to generate paramagnetic five-coordinate iron complexes with P_3Cl_2 donor sets.[14]

The ease with which one of the chloride ligands of complex ***cis*-1** apparently dissociates is probably not only due to the fact that it is *trans* to a phosphine ligand. The related complexes **7**[16] and **8**[17] are diamagnetic under similar conditions. Coordination of bulky tetradentate ligands $P((CH_2)_2PPh_2)_3$ and $P(o\text{-}C_6H_4PPh_2)_3$ to iron(II) chloride has only resulted in the isolation of paramagnetic cationic monochloride cations $[Fe(P((CH_2)_2PPh_2)_3)Cl]^+$ (**10**)[18] and $[Fe(P(o\text{-}C_6H_4PPh_2)_3)Cl]^+$ (**11**),[19] respectively. The existence of monochloride cations **10** and **11** has been attributed to the greater rigidity of the tetradentate ligands in which the chelate bite angles are restricted to 84 ± 2°;[16] however, this rationalization is not consistent with the structure of the dichloride complex **8**[17] in which the chelate bite angles are similarly restricted to 85.8 ± 1°. It is more likely that bulky phosphine ligands are better accommodated in five-coordinate monochloride complexes,[20] and the steric bulk of the BPE5 ligands contributes significantly to the lability of chloride in ***cis*-1**.

Addition of excess phosphine (BPE5, DMPE, or PMe_3) to complex ***cis*-1** in THF solution also suppressed paramagnetism and was accompanied by isomerization of the complex to form an equilibrium mixture of ***cis*-1** and ***trans*-1** (*ca.* 90:10). Addition of DMPE also led to phosphine exchange, and the complex containing one DMPE and one BPE5 ligand [Fe(DMPE)(BPE5)Cl_2] was characterized by NMR spectroscopy (see below). No charged $[FeP_5Cl]^+$ (P = phosphine) cationic complexes were detected in THF solution; however, the cation $[Fe(BPE5)_2(PMe_3)Cl]^+$ (**12**) has been isolated from more polar solvents (see below).

***cis*-1** is stable with respect to *cis/trans* isomerization in the absence of free phosphines, and this suggests that the mechanism of isomerization is probably via chloride dissociation from ***cis*-1** followed by coordination of free phosphine to give a cation of the type $[FeP_5Cl]^+$. Reversible loss of a phosphine donor provides an avenue for isomerization and also ligand exchange.

Chloride Ligand Substitution Reactions of *cis*-Fe(BPE5)$_2$Cl$_2$ (*cis*-1) by Halides. Reaction of complex ***cis*-1** in methanol solution with an excess of the appropriate sodium or potassium halide resulted in almost instantaneous precipitation of the corresponding iron dihalide complexes *cis*-$Fe(BPE5)_2Br_2$ (***cis*-13**) as a dark purple crystalline solid or *trans*-$Fe(BPE5)_2I_2$ (**14**) as a green microcrystalline solid. In both cases, substitution presumably occurs by stepwise reversible dissociation of chloride and association of halide (Br^- or I^-) and the reaction is driven to completion by the precipitation of the insoluble products. Substitution by bromide or iodide was too rapid to allow partially substituted complexes $Fe(BPE5)_2ClX$ to be observed by ^{31}P NMR spectroscopy.

The dibromide complex ***cis*-13** does not exhibit paramagnetic properties like those of complex ***cis*-1**. In refluxing toluene, an equilibrium mixture of ***cis*-13** and ***trans*-13** was established (∼1:1.8) which on cooling reverted to ***cis*-13**. Gentle heating of solid ***cis*-13** to 220 °C gave ***trans*-13** as a green crystalline solid, which on dissolution in toluene gave rise to a green solution that darkened over approximately 20 min and from which ***cis*-13** precipitated. In the solid state ***trans*-13** was air stable and maintained its isomeric integrity over an indefinite period.

The diiodide complex **14** was insoluble in most organic solvents. The isotropic region of the solid-state $^{31}P\{^1H\}$ MAS NMR spectrum of **14** is essentially a singlet resonance with two symmetrical shoulders giving the peak the appearance of a broadened triplet (Figure 2) and demonstrates **14** to be of *trans* geometry. Maricq *et al.*[21] and Wu *et al.*[22] have shown that MAS NMR resonances of crystallographically equivalent but magnetically inequivalent nuclei that are dipolar-coupled exhibit multiplet structure. The isotropic regions of the $^{31}P\{^1H\}$ MAS NMR spectra of ***cis*-1** and ***cis*-13** consist of complicated resonances (Figure 2). The crystal structure of ***cis*-1** (Figure 1) shows the four ^{31}P nuclei to be crystallographically inequivalent and therefore part of an AMQX spin system in the solid state. The extreme insolubility of **14** prevented the growth of crystals suitable for crystallographic analysis.

Chloride Ligand Substitution Reactions of *cis*-Fe(BPE5)$_2$Cl$_2$ (*cis*-1) by CO and PMe$_3$. The cationic complex [*cis*-$Fe(BPE5)_2(CO)(Cl)]^+$ (**15**) was formed when a methanol solution of complex ***cis*-1** was stirred under an atmosphere of CO (Scheme 2). The complex was isolated as its bright yellow tetraphenylborate salt. Displacement of chloride by CO was not observed in less polar solvents such as THF and benzene.

The crystal structure of complex **15** (Figure 3) resembles that of ***cis*-1**. The complex is of slightly distorted octahedral geometry in which the CO and chloride ligands are mutually *cis*. Selected bond lengths and bond angles for complex **15** are reported in Table 3. The P−Fe−P chelation angles of **15** are only slightly smaller than in the dichloride ***cis*-1** (Table 2). The Fe−P bond lengths are longer and the Fe−Cl bond lengths

---

(17) (a) Smernik, R. J. Ph.D. Thesis, University of Sydney, 1996. (b) Field, L. D.; Messerle, B. A.; Smernik, R. J.; Hambley, T. W.; Turner, P. *Inorg. Chem.* **1997**, *36*, 2884.

(18) King, R. B.; Kapoor, R. N.; Saran, M. S.; Kapoor, P. N. *Inorg. Chem.* **1971**, *10*, 1851.

(19) Halfpenny, M. T.; Hartley, J. G.; Venanzi, L. N. *J. Chem. Soc. A* **1967**, 627.

(20) Venanzi, L. N.; *Angew. Chem., Int. Ed. Engl.* **1964**, *3*, 453.

(21) Maricq, M. M.; Waugh, J. S. *J. Chem. Phys.* **1979**, *70*, 3300.

(22) Wu, G.; Wasylishen, R. E. *Inorg. Chem.* **1994**, *33*, 2774 and references therein.

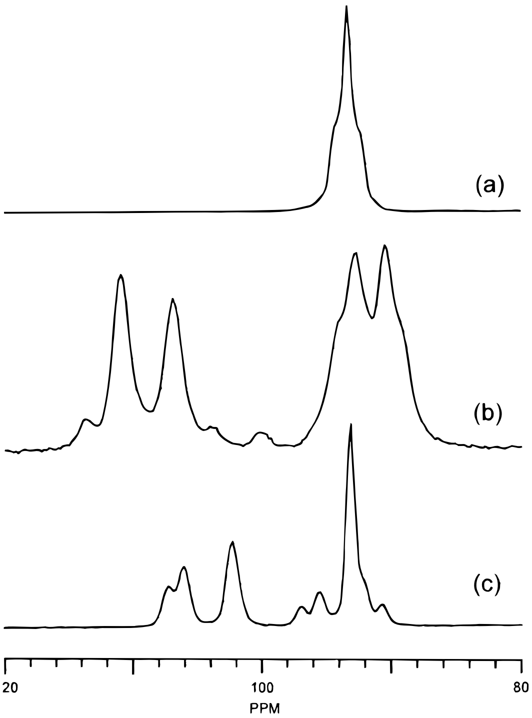

Figure 2. ^{31}P MAS NMR spectra (121 MHz, spin rate 10 kHz): (a) *trans*-Fe(BPE5)$_2$I$_2$ (**14**); (b) *cis*-Fe(BPE5)$_2$Br$_2$ (***cis*-13**); (c) *cis*-Fe(BPE5)$_2$Cl$_2$ (***cis*-1**).

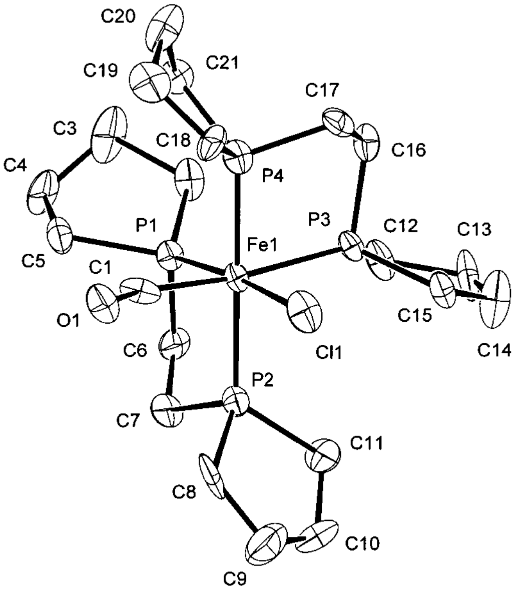

Figure 3. ORTEP plot (25% thermal ellipsoids, non-hydrogen atoms) of the cation [*cis*-Fe(BPE5)$_2$(CO)(Cl)]$^+$ (**15**), BPh$_4$$^-$ salt.

Scheme 2

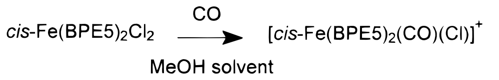

Table 3. Bond Lengths (Å) and Angles (deg) about the Iron Atom of [*cis*-Fe(BPE5)$_2$(CO)(Cl)]$^+$ (**15**)[a]

	Bond Lengths		
Fe(1)−Cl(1)	2.341(9)	Fe(1)−P(2)	2.237(8)
Fe(1)−C(1)	1.93(3)	Fe(1)−P(3)	2.260(7)
Fe(1)−P(1)	2.237(7)	Fe(1)−P(4)	2.231(8)
	Bond Angles		
Cl(1)−Fe(1)−P(1)	174.8(4)	P(1)−Fe(1)−C(1)	90(1)
Cl(1)−Fe(1)−P(2)	89.3(3)	P(2)−Fe(1)−P(3)	96.9(3)
Cl(1)−Fe(1)−P(3)	88.7(3)	P(2)−Fe(1)−P(4)	174.8(3)
Cl(1)−Fe(1)−P(4)	86.3(3)	P(2)−Fe(1)−C(1)	91(1)
Cl(1)−Fe(1)−C(1)	89(1)	P(3)−Fe(1)−P(4)	85.7(3)
P(1)−Fe(1)−P(2)	85.7(3)	P(3)−Fe(1)−C(1)	172(1)
P(1)−Fe(1)−P(3)	92.9(2)	P(4)−Fe(1)−C(1)	87(1)
P(1)−Fe(1)−P(4)	98.7(3)		

[a] Errors in the least significant figures are presented in parentheses.

are shorter in **15** than corresponding bond lengths in ***cis*-1** (Table 2), and this is consistent with the cationic nature of **15**. The phospholane rings adopt almost envelope conformations with minimum torsion angles in each ring of 2° (P(1)), 5° (P(2)), 0° (P(3)), and 6° (P(4)).

Treatment of a methanol solution of complex ***cis*-1** with PMe$_3$ gave an equilibrium mixture of the cationic complexes [*cis*-Fe(BPE5)$_2$(PMe$_3$)(Cl)]$^+$ (***cis*-16**) and [*trans*-Fe(BPE5)$_2$(PMe$_3$)(Cl)]$^+$ (***trans*-16**) (~3:1). The isomers were isolated as the tetraphenylborate salts and could not be separated by fractional recrystallization. The ratio of isomers did not alter on refluxing in methanol (prior to isolation) or in acetone (after isolation). The coordination environments of ***cis-16*** and ***trans*-16** are both [FeP$_5$Cl]$^+$ in which the chloride ligands are necessarily *trans* to phosphine. The greater proportion of ***cis*-16** probably primarily reflects lesser steric encumbrance in this isomer.

In similar reactions, treatment of a methanol solution of ***cis*-1** with the bidentate phosphines BPE5 (**2**) or DEPE resulted in complex mixtures of monomeric and dimeric complexes. No reaction was observed between ***cis*-1** and triphenylphosphine, and this is probably due to the great steric bulk of this phosphine.

Phosphine Ligand Displacement Reactions of *cis*-Fe(BPE5)$_2$Cl$_2$ (*cis*-1). A series of ligand substitution reactions using the bidentate phosphine ligands BPE5 (**2**), DMPE (**17**), DEPE (**18**), and DPrPE (**19**) were performed with complexes ***cis*-1** and **3**−**5** to assess the relative chelation strength of BPE5 (**2**). Ligand substitution was monitored by ^{31}P NMR spectroscopy.

The bidentate phosphines **18** and **19** did not displace BPE5 (**2**) from ***cis*-1**. After prolonged heating at 70 °C, an equilibrium concentration of complex ***trans*-1** was established. At 70 °C, **17** displaced BPE5 (**2**) from ***cis*-1** in approximately 20 min to give Fe(DMPE)$_2$Cl$_2$ (**3**). BPE5 (**2**) readily displaced DEPE and DPrPE ligands from their respective Fe(PP)$_2$Cl$_2$ complexes (**4**, **5**) at ambient temperature, but displacement of DMPE from **3** to give complexes ***cis*-1** and ***trans*-1** was slow at ambient temperature but more rapid at 70 °C. The relative chelation strength of the bidentate phosphines in Fe(PP)$_2$Cl$_2$ complexes is BPE5 ≈ DMPE > DEPE >DPrPE.

Where phosphine substitution occurred, the intermediate mixed-ligand complexes Fe(BPE5)(PP)Cl$_2$ were detected. Complexes Fe(BPE5)(DMPE)Cl$_2$ (**20**) and Fe(BPE5)(DEPE)Cl$_2$ (**21**) are solely *trans* complexes. The predominant isomer of complex Fe(BPE5)(DPrPE)Cl$_2$ (**22**) is also *trans*; however, an unsymmetrically substituted *cis* complex was also detected as a minor product (<5%) and is assigned as *cis*-Fe(BPE5)(DPrPE)Cl$_2$ (***cis*-22**). The propensity for the mixed-ligand complexes **20**−**22** to exhibit *trans* geometries reflects the lesser steric bulk and greater flexibility of the terminal alkyl groups of ligands **17**−**19** compared with BPE5 (**2**); only DPrPE, the bulkiest of the bidentate ligands studied, gives rise to a *cis* mixed-ligand complex (***cis*-22**).

The characteristic ^{31}P{^{1}H} NMR spectra of the AA′XX′ spin

Table 4. ^{31}P NMR Chemical Shifts and Coupling Constants for the AA′XX′ Spin Systems of the Mixed Ligand Complexes $Fe(BPE5)(DMPE)Cl_2$ (**20**), $Fe(BPE5)(DEPE)Cl_2$ (**21**), and $Fe(BPE5)(DPrPE)Cl_2$ (***trans*-22**) and Related Complexes

complex	$\delta(P_{AA'})^a$	$\delta(P_{XX'})^a$	$J_{AA'}$, $J_{XX'}$	$J_{AX} = J_{A'X}$	$J_{AX'} = J_{A'X}$
$Fe(BPE5)(DMPE)Cl_2$	92.84	57.28	+41.2(1), +41.3(3)	+50.2(3)	−144.3(3)
$Fe(BPE5)(DEPE)Cl_2$	87.34	66.18	+40.7(2), +41.0(4)	+47.6(3)	−132.4(3)
$Fe(BPE5)(DPrPE)Cl_2$	87.20	62.43	+41.2(1), +41.3(3)	+46.6(3)	−132.5(3)
$Fe(DMPE)(DEPE)Cl_2{}^b$	67.74	55.78	+40.0(7), +40.2(6)	+50.4(5)	−132.3(7)
$Fe(DMPE)(DPrPE)Cl_2{}^b$	63.25	55.99	+39.9(2), +39.8(2)	+50.2(2)	−132.5(2)
$Fe(DEPE)(DPrPE)Cl_2{}^c$	63.06	57.96	+40.1(3), +40.4(2)	+47.5(2)	−121.4(2)
$Fe(DEPE)(DHPE)Cl_2{}^b$	80.61	9.59	+37.9(3), +44.5(3)	+57.3(2)	−150.8(2)
$Fe(DPrPE)(DHPE)Cl_2{}^b$	75.05	9.41	+37.7(3), +44.0(3)	+56.5(3)	−151.6(3)

[a] Chemical shifts of ligands appear in order, with respect to the complex notation in the left-hand column. $^{31}P\{^1H\}$ NMR spectra were recorded at 162 MHz and 300 K, in THF unless otherwise stated. Chemical shifts (δ) are referenced to external, neat trimethyl phosphite (taken as δ 140.85 ppm). Coupling constants (in Hz, with uncertainties in parentheses) were determined by computer simulation. $J_{AA'}$ and $J_{XX'}$ could not be individually assigned with the available data. The signs of the coupling constants were assigned by analogy with the complexes reported in ref 14. [b] In toluene at 223 K (taken from ref 14). [c] 223 K (taken from ref 14).

systems of **20**, **21**, and ***trans*-22** were simulated[23] to establish the chemical shifts and coupling constants of the mixed-ligand systems (Table 4).

Conclusions

The BPE5 ligand **2** is a strongly chelating ligand of similar chelation strength to DMPE (**17**) in $Fe(PP)_2Cl_2$ complexes. The relatively rigid steric bulk of **2** is probably responsible for the tendency of the $Fe(BPE5)_2X_2$ (X = halide) and $[Fe(BPE5)_2(L)Cl]^+$ (L = phosphine or CO) complexes to exhibit *cis* coordination geometries. The crystal structures of ***cis*-1** and **15** show that the presence of two BPE5 diphospholane ligands significantly crowds the remaining two coordination sites. One chloride ligand of *cis*-$Fe(BPE5)_2Cl_2$ (***cis*-1**) is notably labile probably due to the steric bulk of the diphospholane ligands in the complex and also because it is located *trans* to a phosphine ligand. The reversible dissociation of chloride from ***cis*-1** accounts for the observed temperature-dependent paramagnetism and for the ease with which one chloride can be substituted by other ligands.

Experimental Section

All manipulations of air-sensitive phosphines, metal complexes, and reagents were carried out using standard Schlenk or vacuum techniques[24] or in a Vacuum Atmospheres argon-filled drybox.

Anhydrous iron(II) dichloride was prepared by following the procedure of Leigh *et al.*[25] The phosphines DMPE (**17**), DEPE (**18**), and DPrPE (**19**) were purchased from Strem and used without further purification. The iron complexes $Fe(DMPE)_2Cl_2$ (**3**), $Fe(DEPE)_2Cl_2$ (**4**), and $Fe(DPrPE)_2Cl_2$ (**5**) were prepared by literature methods.[26] The ligand BPE5 was prepared as described previously.[12]

Diethyl ether, tetrahydrofuran, benzene, and toluene were stored over sodium wire and were distilled under nitrogen from sodium benzophenone ketyl[27] immediately prior to use. Absolute methanol was distilled from magnesium turnings.[28] NMR solvents were obtained from Merck and Cambridge Isotopes and were used as supplied (methanol-d_4 and acetone-d_6) or degassed by at least three freeze−pump−thaw cycles before distillation from potassium benzophenone ketyl under static high-vacuum conditions (toluene-d_8). All bulk compressed gases were obtained from British Oxygen Co. (BOC Gases). Argon (>99.99%), nitrogen (>99.5%), and carbon monoxide (>99.5%) were used as supplied without further purification.

Mass spectra of organometallic complexes were recorded on a Finnigan MAT TSQ-46 mass spectrometer (San Jose, CA) fitted with a desorption probe and using chemical ionization (CI, UHP methane > 99.999% or UHP ammonia > 99.999%) with a source temperature of 140 °C and an electron energy of 100 eV. Data are quoted in the form *x* (*y*), where *x* is the mass/charge ratio (*m/z*) and *y* is the percentage abundance relative to the base peak. Mass spectra were recorded scanning mass ranges greater than that of the free phosphine ligand, typically *m/z* > 250. Peaks of low intensity are not quoted unless deemed significant.

Infrared spectra were obtained on a Perkin-Elmer 1600 series FTIR spectrophotometer. Melting points were determined using a Gallenkamp melting point apparatus and are uncorrected. Melting points of air-sensitive compounds were performed in capillary tubes sealed under argon. Microanalyses were carried out at the University of New South Wales, Sydney, Australia.

^{1}H, ^{31}P, and ^{13}C NMR spectra were recorded on a Bruker AMX400 NMR spectrometer at 400.13, 161.98, and 100.61 MHz, respectively, or on a Bruker AMX600 NMR spectrometer at 600.13 MHz (^{1}H) and 242.94 MHz (^{31}P). All spectra were recorded at 300 K unless otherwise stated. ^{1}H and ^{13}C NMR spectra are referenced to residual solvent resonances. ^{31}P NMR spectra are referenced to external neat trimethyl phosphite taken as 140.85 ppm at the temperature quoted. Chemical shifts (δ) are quoted in ppm with the downfield direction being taken as positive. For [*cis*-$Fe(BPE5)_2(CO)(Cl)][BPh_4]$ **(15)**, the four distinct P nuclei were not unambiguously assigned but they were labeled P_A-P_D for the purpose of reporting shifts and coupling constants, with P_A and P_C being mutually *trans*. Solid-state ^{31}P MAS NMR spectra were recorded on a Bruker MSL300 NMR spectrometer at 121.44 MHz at 293 K with a spin rate of 10 kHz. Spectra were referenced to $NH_4H_2PO_4$ taken as δ 1.00 ppm.

***cis*-Fe(BPE5)$_2$Cl$_2$ (*cis*-1).** A solution of BPE5 (**2**) (721 mg, 3.57 mmol) in THF (~5 mL) was added dropwise over 20 min to a solution of iron(II) chloride (226 mg, 1.78 mmol) in THF (~15 mL). Upon addition, the solution turned dark red. The mixture was stirred for 30 min and ***cis*-1** was precipitated from solution. The crude product was isolated by filtration and recrystallized fromTHF/methanol to give ***cis*-1** as a maroon crystalline solid, mp dec > 119 °C. Yield: 728 mg (77%). $^{31}P\{^1H\}$ NMR (162 MHz, methanol-d_4, 233 K): 93.2, 106.7 (apparent triplets, splitting = 40.0 Hz) ppm. $^1H\{^{31}P\}$ NMR (400 MHz, methanol-d_4, 233 K): 1.36, 1.72, 2.05, 2.17 (8H, 2 $PC\mathbf{H_2}C\mathbf{H_2}P$), 1.44−2.20 (m, 28H), 2.80 (m, 2H), 3.76 (m, 2H) ppm. $^{13}C\{^1H,^{31}P\}$ NMR (100 MHz, methanol-d_4, 233 K): 26.6, 26.9, 27.1, 27.4, 28.4, 28.5, 29.2, 30.0, 31.6, 33.6 ($\mathbf{C}H_2$) ppm. MS (CI, NH_3): *m/z* > 400, 548 (10%, $[Fe(BPE5)_2{}^{35}Cl_2]NH_3{}^+$), 533 (56, $[Fe(BPE5)_2{}^{35}Cl^{37}Cl]H^+$), 531 (63, $[Fe(BPE5)_2{}^{35}Cl_2]H^+$), 497 (34, $[Fe(BPE5)_2{}^{37}Cl]^+$), 496 (24, $[Fe(BPE5)_2{}^{35}Cl]H^+$), 495 (100, $[Fe(BPE5)_2{}^{35}Cl]^+$), 460 (23, $[Fe(BPE5)_2]^+$), 425 (23); *m/z* > 300, 348 (65, $[Fe(BPE5)^{35}Cl^{35}Cl]NH_4{}^+$), 346 (100,

---

(23) Simulations were performed using the computer program PANIC, *P*arameter *A*djustment in *N*MR by *I*teration and *C*alculation (Bruker Spectrospin Pty Ltd.), executed on a Bruker ASPECT 3000 data station.

(24) Shriver, D. F.; Drezdzon, M. A. *The Manipulation of Air Sensitive Compounds*; John Wiley & Sons: New York, 1986.

(25) Hughes, D. L.; Leigh, G. J.; Jimenez-Tenorio, M.; Rowley, A. T. *J. Chem. Soc., Dalton Trans.* **1993**, 75.

(26) Burt, R. J.; Hussain, W.; Leigh, G. J. *J. Organomet. Chem.* **1979**, *182*, 203.

(27) Perrin, D. D.; Armarego, W. L. F. *Purification of Laboratory Chemicals*, 3rd ed.; Pergamon Press: London, 1988.

(28) Furnis, B. S.; Hannaford, A. J.; Smith, P. W. G.; Tatchell, A. R. *Vogel's Textbook of Practical Organic Chemistry*, 5th ed.; Longmans: London, 1989.

[Fe(BPE5)^{35}Cl$_2$]NH$_4^+$). Anal. Calcd for $C_{20}H_{40}P_4Cl_2Fe$: C, 45.22; H, 7.59. Found: C, 45.0; H, 7.8.

cis*-Fe(BPE5)$_2$Br$_2$ (*cis*-13).** A deep red solution of ***cis*-1** (275 mg, 518 mol) in methanol (∼10 mL) was treated with a solution of lithium bromide (88 mg, 2.1 mmol, ∼4 equiv) in methanol (∼2 mL). The color of the solution turned dark purple almost immediately, and a purple crystalline solid precipitated from solution. The crude product was recrystallized from hot toluene to give *cis*-Fe(BPE5)$_2$Br$_2$·H$_2$O (cis*-13**) as large purple air-stable cubic crystals, mp dec > 306 °C. Yield: 238 mg (75%). ^{31}P{^{1}H} NMR (162 MHz, toluene-d_8): 86.7, 106.6 (apparent triplets, splitting = 37.5 Hz) ppm. ^{1}H{^{31}P} NMR (400 MHz, toluene-d_8): 0.89 (m, 2H), 1.03 (m, 2H), 1.08 (m, 2H), 1.42 (m, 2H), 1.56−1.81 (m, 12H), 1.87 (m, 2H), 1.91−2.37 (m, 16H), 3.82 (m, 2H) ppm. ^{13}C{^{1}H,^{31}P} NMR (100 MHz, toluene-d_8): 27.2, 28.4, 28.5, 28.6, 29.3, 30.1, 30.2, 32.4, 32.7, 34.4 (**C**H$_2$) ppm. MS (CI, CH$_4$): *m/z* > 350, 623 (9, [Fe(BPE5)$_2$^{81}Br$_2$]H$^+$), 622 (33, [Fe(BPE5)$_2$^{81}Br$_2$]$^+$), 621 (23, [Fe(BPE5)$_2$^{79}Br^{81}Br]H$^+$), 620 (73, [Fe(BPE5)$_2$^{79}Br^{81}Br]$^+$), 619 (17, [Fe(BPE5)$_2$^{79}Br$_2$]H$^+$), 618 (45, [Fe(BPE5)$_2$^{79}Br$_2$]$^+$), 542 (23, [Fe(BPE5)$_2$^{81}Br]H$^+$), 541 (89, [Fe(BPE5)$_2$^{81}Br]$^+$), 540 (28, [Fe(BPE5)$_2$^{79}Br]H$^+$), 539 (100, [Fe(BPE5)$_2$^{79}Br]$^+$), 420 (21, [Fe(BPE5)^{81}Br$_2$]$^+$), 418 (44, [Fe(BPE5)^{79}Br ^{81}Br$_2$]$^+$), 416 (25, [Fe(BPE5)^{79}Br$_2$]$^+$). Anal. Calcd for $C_{20}H_{40}P_4Br_2Fe{\cdot}H_2O$: C, 37.64; H, 6.64. Found: C, 37.7; H, 6.9.

***trans*-Fe(BPE5)$_2$Br$_2$ (*trans*-13).** A round bottom flask containing dark purple crystals of anhydrous ***cis*-13** (65 mg, 100 mol) was heated gently to 225 °C under vacuum (to prevent aerial oxidation). At 220−221 °C, the solid turned green and ***trans*-13** was isolated as a bright green air stable solid, mp dec > 306 °C. Yield: 65 mg (100%). ^{31}P{^{1}H} NMR (162 MHz, toluene-d_8): 92.5 (s) ppm. ^{1}H{^{31}P} NMR (400 MHz, toluene-d_8): 1.90−2.12 (m, 24H), 2.22 (s, 8H, PC**H$_2$**C**H$_2$**P), 2.38 (m, 8H) ppm. ^{13}C{^{1}H,^{31}P} NMR (100 MHz, toluene-d_8): 28.8, 29.1 (P**C**H$_2$**C**H$_2$), 31.0 (P**C**H$_2$**C**H$_2$P) ppm.

***trans*-Fe(BPE5)$_2$I$_2$ (14).** A deep red solution (∼10 mL) of ***cis*-1** (103 mg, 194 mol) in methanol (∼10 mL) was treated with a solution of excess sodium iodide (120 mg, 800 mol, ∼4 equiv) in methanol (∼2 mL). The color of the solution turned royal blue, and a green solid was precipitated within 30 s. The solid was isolated by filtration and washed with methanol to give *trans*-Fe(BPE5)$_2$I$_2$ (**14**) as a green microcrystalline solid, mp dec > 352 °C. Yield: 71 mg (64%). ^{31}P{^{1}H} MAS NMR (121 MHz, 293 K): 93.2 ppm. MS (CI, CH$_4$): *m/z* > 350, 715 (22%, [Fe(BPE5)$_2$I$_2$]H$^+$), 714 (100, [Fe(BPE5)$_2$I$_2$]$^+$), 588 (24, [Fe(BPE5)$_2$I]H$^+$), 587 (53, [Fe(BPE5)$_2$I]$^+$), 513 (12, [Fe(BPE5)I$_2$]H$^+$), 512 (30, [Fe(BPE5)I$_2$]$^+$), 384 (42, [Fe(BPE5)I]$^+$). Anal. Calcd for $C_{20}H_{40}P_4I_2Fe$: C, 33.64; H. 5.65. Found: C, 33.6; H, 5.9.

[*cis*-Fe(BPE5)$_2$(CO)(Cl)][BPh$_4$] (15). A solution of ***cis*-1** (98 mg, 180 mol) in methanol (∼5 mL) was stirred under an atmosphere of carbon monoxide for approximately 30 min. The color of the deep red solution gradually turned yellow. A yellow solid was precipitated from solution on addition of excess sodium tetraphenylborate in methanol. The crude product was isolated by filtration and recrystallized from acetone to give [*cis*-Fe(BPE5)$_2$(CO)(Cl)]$^+$BPh$_4^-$ (**15**) as a yellow, air-stable microcrystalline solid, mp dec > 303 °C. Yield: 136 mg (96%). Cation **15** was also synthesized in methanol-d_4 and was characterized by NMR spectroscopy without isolation. ^{31}P{^{1}H} NMR (243 MHz, methanol-d_4, 233 K): 80.5 (1P, ddd, $^2J_{P(A)-P(D)} = 40.0$ Hz, $^2J_{P(B)-P(D)} = 60.0$ Hz, $^2J_{P(C)-P(D)} = 53.2$ Hz, **P**$_D$), 87.2 (1P, ddd, $^2J_{P(B)-P(C)} = 23.6$ Hz, $^2J_{P(A)-P(C)} = 106.3$ Hz, **P**$_C$), 92.2 (1P, ddd, $^2J_{P(A)-P(B)} = 33.3$ Hz, **P**$_B$), 93.0 (1P, ddd, **P**$_A$) ppm. ^{1}H{^{31}P} NMR (600 MHz, methanol-d_4, 233 K): 1.46, 1.48, 1.89, 2 2.04, 2.10, 2.20, 2.28 ppm (8H, 2 PC**H$_2$**C**H$_2$**P); 1.51−2.17 ppm (m, 28H, C**H$_2$**); 2.33 (m, 1H, CH**H**), 2.39 (m, 1H, CH**H**), 2.60 (m, 2H, C**H$_2$**) ppm. ^{13}C{^{1}H,^{31}P} NMR (100 MHz, methanol-d_4, 233 K): 26.8, 27.0, 27.4, 27.5, 27.7, 27.8, 28.5, 28.6, 2 28.7, 29.2, 29.4, 29.5, 29.7, 30.1, 30.3, 30.4, 31.0, 31.7, 32.4 (**C**H$_2$), 185.0 (**C**O) ppm. MS (CI, CH$_4$): *m/z* > 400, 523 (3%, [Fe(BPE5)$_2$(CO)^{35}Cl]$^+$), 498 (4, [Fe(BPE5)$_2$^{37}Cl]H$^+$), 497 (20, [Fe(BPE5)$_2$^{37}Cl] $^+$), 496 (20, [Fe(BPE5)$_2$^{35}Cl]H$^+$), 495 (67, [Fe(BPE5)$_2$^{35}Cl]$^+$), 489 (56, [Fe(BPE5)$_2$(CO)]H$^+$), 488 (100, [Fe(BPE5)$_2$(CO)]$^+$), 461 (7, [Fe(BPE5)$_2$]H$^+$), 460 (4, [Fe(BPE5)$_2$]$^+$). IR (ν_{max}, Nujol): 1965 (s, CO) cm^{-1}. Anal. Calcd for $C_{45}H_{60}P_4BClOFe$: C, 64.12; H, 7.18. Found: C, 63.7; H, 7.1.

Table 5. Crystal data for *cis*-Fe(BPE5)$_2$Cl$_2$ (***cis*-1**) and [*cis*-Fe(BPE5)$_2$(CO)(Cl)][BPh$_4$] (**15**)

	cis-Fe(BPE5)$_2$Cl$_2$ (***cis*-1**)	[*cis*-Fe(BPE5)$_2$(CO)-(Cl)][BPh$_4$] (**15**)
empirical formula	$C_{24}H_{48}Cl_2FeP_4O$	$C_{45}H_{60}BClFeO_{1.25}P_4$
fw, g mol^{-1}	603.29	846.97
space group	$P2_1/n$ (#14)	$P2_1$/a (#14)
a, Å	12.084(3)	12.938(3)
b, Å	14.059(2)	29.647(4)
c, Å	17.665(2)	13.131(3)
β, deg	101.77(1)	107.89(2)
cell vol, Å^3	2938.0(8)	4793(2)
calcd density, g cm^{-3}	1.364	1.174
Z	4	4
λ(Cu Kα), Å	1.541 78	1.541 78
μ, cm^{-1}	79.66	45.30
$R(F_o)^a$	0.072	0.092
$R_w(F_o)^a$	0.068	0.087

[a] $R = \sum(||F_o| - |F_c||)/\sum|F_o|$; $R_w = (\sum w(|F_o| - |F_c|)^2/\sum wF_o^2)^{1/2}$; $w = 1/\sigma^2(F_o)$.

[Fe(BPE5)$_2$(PMe$_3$)(Cl)][BPh$_4$] (16). Trimethylphosphine (20 mg, 270 mol, 1.4 equiv) was condensed into a solution of ***cis*-1** (100 mg, 188 mol) in methanol (∼5 mL). The deep red solution turned pale red, from which a dark pink solid was precipitated on addition of excess sodium tetraphenylborate in methanol. Recrystallization of the precipitate from acetone gave [Fe(BPE5)$_2$(PMe$_3$)Cl][BPh$_4$] (**16**) as a pink microcrystalline solid consisting of two isomers ***cis*-16** and ***trans*-16** (∼3:1), mp dec > 228 °C. Yield: 162 mg (97%). ^{31}P{^{1}H} NMR (162 MHz, acetone-d_6): ***cis*-16**, 9.7 (1P, complex m, **P**Me$_3$) 85.8 (2P, complex m), 88.6 (1P, complex m), 93.4 (1P, complex m) ppm; ***trans*-16**, 24.5 (1P, p, $^2J_{P-PMe_3} = 48.8$ Hz, **P**Me$_3$), 91.0 (4P, d) ppm. ^{1}H{^{31}P} NMR (400 MHz, acetone-d_6): ***cis*-16**: 1.58−2.47 (m, −C**H$_2$**−), 1.75 (s, 9H, P(C**H$_3$**)$_3$), 6.92 (m, 4H, BAr**H*$_{para}$***), 7.07 (m, 8H, BAr**H*$_{meta}$***), 7.48 (m, 8H, BAr**H*$_{ortho}$***) ppm. ^{13}C{^{1}H,^{31}P} NMR (100 MHz, acetone-d_6): 22.7 (d, $^1J_{P-Me} = 21.0$, P**C**H$_3$), 26.2, 26.6, 27.0, 27.9, 28.0, 28.6, 28.7, 28.8, 29.0, 29.0, 29.0, 29.1, 29.4, 30.7, 32.0, 31.4, 31.7, 32.3, 33.3, 34.3 (**C**H$_2$), 122.6 (Ar**C*$_{para}$*** BPh$_4^-$), 126.3 (Ar**C*$_{ortho}$***, BPh$_4^-$), 137.5 (Ar**C*$_{meta}$***, BPh$_4^-$), 165.5 (m, Ar**C*$_{ipso}$***, BPh$_4^-$) ppm. MS (CI, CH$_4$): *m/z* > 400, 572 (1%, [Fe(BPE5)$_2$(PMe$_3$)^{35}Cl]$^+$), 537 (9, [Fe(BPE5)$_2$(PMe$_3$)]H$^+$), 536 (8, [Fe(BPE5)$_2$(PMe$_3$)]$^+$), 498 (10, [Fe(BPE5)$_2$37Cl]H$^+$), 497 (37, [Fe(BPE5)$_2$^{37}Cl]$^+$), 496 (25, [Fe(BPE5)$_2$^{35}Cl]H$^+$), 495 (100, [Fe(BPE5)$_2$^{35}Cl]$^+$). Anal. Calcd for $C_{47}H_{69}P_5BClFe$: C, 63.35; H, 7.80. Found: C, 63.1; H, 7.9.

X-ray Crystallography. The crystal data for complexes ***cis*-1** and **15** are reported in Table 5. The crystals of each complex (***cis*-1** and **15**) were obtained by slow evaporation of THF/methanol and acetone solutions, respectively. Crystals of each complex were inserted into glass capillaries and mounted on a Rigaku AFCR7 diffractometer employing a graphite-monochromated Cu Kα radiation.

Primitive monoclinic cell constants for the dichloride complex ***cis*-1** were obtained from a least-squares refinement using the setting angles of 25 reflections in the range $19.47 < 2\theta < 27.36°$. ω scans of several intense reflections, made prior to data collection, had an average width at half-height of 0.16°. Data were collected with $\omega/2\theta$ scans ($0.79 + 0.35 \tan\theta$) at a speed of 32.0°/min (ω). The weak reflections ($I < 15.0\sigma(I)$) were rescanned (maximum of 10 scans), and the counts were accumulated. Stationary background counts were recorded on each side of the reflection, and the ratio of peak counting time to background counting time was 2:1. The intensities of three representative reflections measured every 150 reflections decreased by 10.1%, and accordingly a linear correction was applied to the data. An empirical absorption correction based on azimuthal scans of three reflections resulted in transmission factors ranging from 0.84 to 0.99. The data were corrected for Lorentz and polarization effects, and a small correction for secondary extinction was also applied (coefficient = 2.44×10^{-6}).

Primitive monoclinic cell constants for complex **15** were obtained from a least-squares refinement using the setting angles of 25 reflections in the range $20.37 < 2\theta < 40.00°$. ω scans of several intense reflections, made prior to data collection, had an average width at half-height of 0.33°. Data were collected with $\omega/2\theta$ scans ($1.00 + 0.35 \tan\theta$) at a speed of 8.0°/min (ω). The weak reflections ($I < 15.0\sigma(I)$)

were rescanned up to 10 times, and the counts were accumulated. Background counts were calculated using a Lehmann–Larsen routine.[29] The intensities of three representative reflections measured every 150 reflections did not change significantly during the data collection. An analytical absorption correction was applied to the data, and the data were also corrected for Lorentz and polarization effects.

In the crystals of **1** and **15**, both enantiomers were observed and the crystals contain racemic mixtures. All calculations were performed using the teXsan[30] crystallographic software package. The structures were solved by direct methods[31] and expanded using Fourier techniques.[32] With the exception of a solvate oxygen in complex **15**, the non-hydrogen atoms were refined anisotropically and the hydrogen atoms were included in the full-matrix least-squares refinement at calculated positions with group temperature factors. In complex **15**, no hydrogen atoms were attached to the solvate oxygen atom, the population of which was initially refined and then fixed at 0.25. The refinements converged, with the largest parameter shift to estimated standard deviation ratio being 0.01 in both cases. The structure of complex **15** is of poor quality, with the carbonyl group being particularly ill-defined. The short C═O bond and the near nonpositive definite nature of the carbonyl carbon may simply reflect the poor crystal quality but may also be the result of a minor mixed occupancy of the carbonyl and chloro sites. Neutral atom scattering factors were taken from Cromer and Waber.[33] Anomalous dispersion effects were included in the structure factor calculation,[34] and the values for $\Delta f'$ and $\Delta f''$ were those of Creagh and McAuley.[35a] The values for the mass attenuation coefficients are those of Creagh and Hubbell.[35b]

Acknowledgment. We gratefully acknowledge financial support from the Australian Research Council.

Supporting Information Available: X-ray crystallographic files, in CIF format, for complexes *cis*-Fe(BPE5)$_2$Cl$_2$ (***cis*-1**) and [*cis*-Fe(BPE5)$_2$(CO)(Cl)][BPh$_4$] (**15**) are available on the Internet only. Access information is given on any current masthead page.

IC9701928

---

(29) Lehman, M. S.; Larsen, F. K. *Acta Crystallogr.* **1974**, *A30*, 580.

(30) teXsan: *Crystal Structure Analysis Package*; Molecular Structure Corp.: The Woodlands, TX, 1985, 1992.

(31) SIR92: Altomare, A.; Burla, M. C.; Camalli, M.; Cascarano, M.; Giacovazzo, C.; Guagliardi, A.; Polidori, G. *J. Appl. Crystallogr.* **1993**, *26*, 343.

(32) DIRDIF94: Beurskens, P. T.; Admiraal, G.; Beurskens, G.; Bosman, W. P.; de Gelder, R.; Israel, R.; Smits, J. M. M. *The DIRDIF-94 program system*; Technical Report of the Crystallography Laboratory; University of Nijmegen: Nijmegen, The Netherlands, 1994.

(33) Cromer, D. T.; Waber, J. T. *International Tables for X-ray Crystallography*; The Kynoch Press: Birmingham, England, 1974; Vol. IV, Table 2.2 A.

(34) Ibers, J. A.; Hamilton, W. C. *Acta Crystallogr.* **1964**, *17*, 781.

(35) (a) Creagh, D. C.; McAuley, W. J. *International Tables for Crystallography*; Kluwer Academic Publishers: Boston, MA, 1992; Vol. C, Table 4.2.6.8, pp 219–222. (b) *Ibid.*, Table 4.2.4.3, pp 200–206.